Theory of the late-stage crystallization of eutectic composition melts

S.A. Kukushkin*, D.A. Grigoriev

Institute of Mechanical Engineering Problems, Russian Academy of Sciences, Bolshoj 61, V.O., St. Petersburg 199178, Russian Federation

Abstract

A theory of late-stage crystallization in eutectic point of binary eutectic melts whose pure components have close melting points is developed. A complete system of equations describing the evolution of an ensemble of nuclei has been obtained. An asymptotic solution to this system of equations shows that there is a strong correlation between precipitates of a different composition, which is related to specific features of the eutectic systems. The main characteristics of dispersed systems of eutectic composition including the distribution function, the critical size and the time dependence of density of nuclei have been found. The effect of heat removal from the system on these characteristics and on the structure of the final solid product has also been studied. Our theoretical results have been confirmed by experimental data. © 2000 Elsevier Science Ltd. All rights reserved.

Keywords: Eutectic melts; Late-stage crystallization; Critical size

1. Introduction

Crystallization of eutectic systems has been studied in numerous publications summed up in monographs [1,2]. The interest in these systems stems primarily from the fact that many materials employed widely in metallurgy, microelectronics and superconductor technology are of the eutectic type [1–4]. Fig. 1 presents a typical and the simplest eutectic-phase diagram [2].

Previous studies on the crystallization of eutectic melts indicate that depending on the actual kind of the phase diagram, melts crystallize either in a mixture of finely dispersed crystals of pure components A and B (see Fig. 1), or in the form of plates or rods, for example, of material A in matrix B. In some cases, the eutectic melts can solidify to a glassy state or form dendrite structures.

Many attempts for explaining the diversity of the structures obtained were developed [1–4]. No clear answer to this problem appears to exist yet.

The melt crystallization processes are known to be typical first-order phase transitions. Any phase transition runs through several stages [5]. In the first stage, nuclei of the new phase appear. In the second, these nuclei grow without a change in their number. The final stage is the coalescence or Ostwald ripening [5]. This work is aimed at describing the process of Ostwald ripening occurring in crystallization of the melts of eutectic composition.

A theory of late-stage crystallization (or of Ostwald ripening) of binary alloys and, in particular, of melts having state diagram of the eutectic type, whose simplest view is represented in Fig. 1, was developed in Ref. [6]. The above publication considered only, however, the process that occurred either to the left of the eutectic point or to the right of it. Only a qualitative analysis of the crystallization of the eutectic melts was attempted in Ref. [6]. This work is aimed at constructing a quantitative theory of late-stage crystallization of the eutectic melts. We will start with the consideration of conservative systems to be followed by open ones.

2. Conservative systems: formulation of the problem and physical essence of the process

Let us consider a binary melt consisting of components A and B (which in a general case can be individual substances

* Corresponding author. Tel.: +7-812-321-47-77; fax: +7-812-321-47-71.

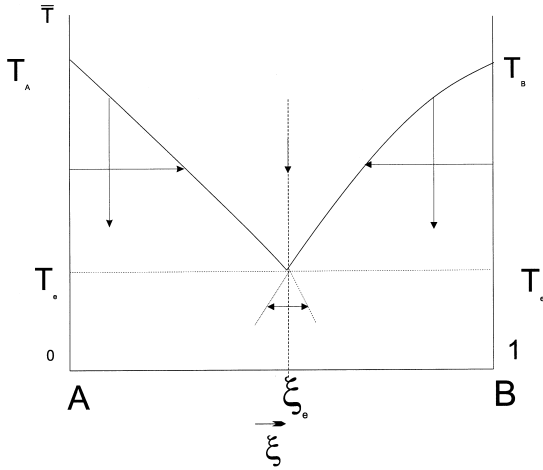   *E-mail address:* ksa@ipme.ru (S.A. Kukushkin).

Fig. 1. Typical diagram of state for an eutectic system of components A and B. T_A and T_B are the melting points of the pure components, ξ_e is the composition corresponding to the eutectic point, T_e is the temperature of crystallization of a eutectic melt, and the arrows show possible crystallization paths. The lines below the eutectic point identify metastable states.

as well as chemical compositions not breaking down at the temperatures under study), and having a phase diagram of the eutectic type (Fig. 1).

Note that the crystallization of an eutectic melt can be initiated in the following ways. One may either cool the system from the left, i.e. from the direction of the component A, until the system reaches the point corresponding to the composition ξ_e and the component B precipitates, or approach the same point from the right, from the direction of the component B (see Fig. 1). There is, however, another possibility. We may cool a melt exactly of the eutectic composition to a temperature below the eutectic point where nuclei of the new phase are created. Obviously enough, the structure of the eutectic should depend on the way by which it has been formed. If we move to the eutectic point from the left (or right), the melt will already contain crystals of the components A or B. The closer the starting composition of the melt is to that of the pure components, the larger will be the fraction of the total volume occupied by these crystals at the eutectic point compared to the secondary nucleated crystals, i.e. to the crystals A if the component B crystallized initially, or to the crystals B if the component A was the first to crystallize.

These secondary crystals can form obviously by the mechanism of heterogeneous nucleation on the surface of the already existing and growing crystals. Thus, the structure of the forming eutectic depends essentially both on the actual path of its formation and on the initial conditions, i.e. on the composition of the melt from which it was produced by cooling.

We will restrict our consideration here only to the crystallization of melts of exactly the eutectic composition, using

as a case in point the so-called "normal" eutectics, by which one understands the eutectic systems whose components, in a pure form, have similar melting temperatures [2]. In the case where the melting points of the pure components making up the melt differ dramatically melt crystallization results in an anomalous eutectic [2]. In the future, we intend to investigate other crystallization paths for eutectic melts as well as for anomalous eutectics.

Considering the cooling of a melt having the exact eutectic composition below the equilibrium temperature of crystallization of the eutectic, intense nucleation of two groups of nuclei is expected to set in, namely, of nuclei of the compositions A and B. As we have already pointed out, solidification of eutectic melts leads to the formation of a variety of structures [2]. We shall assume for the sake of simplicity that the nuclei are either spheres of radius R, or cylindrical rods of radius R and length l. Then, we isolate the system thermally. Like any system undergoing a first-order transition, our system will eventually reach the stage of Ostwald ripening [6]. This process is accompanied by the creation of a diffusion-controlled thermal field determined by the whole ensemble of particles [6]. Nuclei with radii above the critical value, $R > R_c$, will grow in this field, and those with radii below this level, $R < R_c$, will dissolve.

The evolution of such nuclei on both the left- and the right-hand sides of the diagram in Fig. 1 was discussed in detail in Refs. [6,7]. This theory leads to the following system of equations for spherically symmetric nuclei:

$$\frac{\partial f_i(R,t)}{\partial t} + \frac{\partial}{\partial R}[f_i(R,t)V_{Ri}] = 0, \qquad f_i|_{t=0}(R,t) = f_{0i}, \quad (1)$$

$$\frac{d\bar{\xi}_i}{dt} + 4\pi \int_0^\infty f_i(R,t)J_{D,R,i}R^2 \, dR = 0, \qquad (2)$$

$$\frac{d(\bar{T}c_{pi}\rho_i)}{dt} - 4\pi \int_0^\infty f_i(R,t)J_{T,R,i}R^2 \, dR = 0, \qquad (3)$$

$$L_i J_{D,i} = J_{T,R,i}, \qquad (4)$$

$$T_{Ri} = \varphi_i(\xi_{Ri}), \qquad (5)$$

where Eq. (1) is the equation of continuity for the size distribution function of the new-phase nuclei, $f_i(R,t)$, normalized to the number of nuclei per unit melt volume, $N_i(t) \int_0^\infty f_i(R,t)R^3 \, dR$; Eqs. (2) and (3) describe, respectively, the variation of the average component concentration and temperature in the melt; Eq. (4) connects the heat and matter flows on the boundary of a nucleus of radius R (calculated in Ref. [7]); Eq. (5) relates the equilibrium temperature at the boundary of a nucleus of radius R to composition ξ_{Ri}; $J_{D,R,i}$, $J_{T,R,i}$ are, respectively, the flow of the dissolved component to a new-phase nucleus and the heat flow released in crystallization of a nucleus of radius R; c_{pi} and ρ_{Li} are the specific heat and density of the melt at constant pressure; and $\varphi_i(\xi_{Ri})$ depends on the actual phase diagram of

state and determines the dependence of the equilibrium concentration at the boundary of a nucleus of radius R on temperature. The subscript i identifies the part of the diagram in consideration and, accordingly, the composition of the new-phase nuclei. If we are in the left-hand part of the diagram, where nuclei of composition A form, we can set, for e.g. $i = 1$, and if we are in its right-hand part, and the nuclei have composition B, then $i = 2$. At the eutectic point, the melt contains, simultaneously, nuclei of both components A and B. Since at this point the derivative $(\partial T_0/\partial \xi_0)$ (where T_0 and ξ_0 are, respectively, the equilibrium temperature and equilibrium concentration at the liquidus line) reverses its sign, the growth of the nuclei, as shown qualitatively in Ref. [5], will occur in a correlated way[1]. Indeed, at the eutectic point both types of nuclei of compositions A and B will grow, and in the process change the melt concentration of the components they are made of, and, hence, that of the others as well. For example, the growth of a nucleus of composition A raises the concentration of component B, thus accelerating the rate of its growth. At the same time the increase in the growth rate of nucleus B reduces the concentration of this component in the melt, which, in its turn, accelerates the growth of nuclei A, making the growth of particles of both phases correlated. Obviously enough, the fluxes of the two components will be equal in magnitude but opposite in direction, $J_{D,R,1} = -J_{D,R,2}$. Thus the average concentration in the system will tend to the unified value, namely, the eutectic concentration ξ_e. Note, however, that this is valid only for the case when the equilibrium concentration lines approaching the region of metastable state (Fig. 1) are strictly symmetric about to the eutectic composition line. If this is not the case, the compositional fluctuations may set in the initial stage of nucleus ripening, and the nuclei grow independently as their individual supersaturation is removed in an uncorrelated way. In doing so, their evolution should be considered similar to that of a multiphase system [7]. In the asymptotic region, however, i.e. where supersaturation $\Delta_i \rightarrow 0$, (the condition determining Ostwald ripening), in the immediate vicinity of the eutectic point the metastable lines of equilibrium concentrations will pass practically at an equal distance from the eutectic concentration line [1–4].

Thus in the stage of Ostwald ripening of the new phase nuclei the average concentration $\bar{\xi}$ of components of the eutectic composition remains constant for the system as a whole, and Eq. (2) becomes identically equal to zero (which is certainly not true for the initial stage).

Relation (5) determines therewith the degree of supercooling of the melt with respect to the eutectic temperature T_e. The supercooling of the melt becomes unitary for the whole system.

---

[1] It should be pointed out that we are dealing here only with "normal" eutectics.

3. Basic system of equations for the late-stage crystallization of melts of the eutectic composition

The above reasoning permits us to recast Eqs. (2)–(5) to the form

$$\frac{\partial f_i(R,t)}{\partial t} + \frac{\partial}{\partial R}[f_i(R,t)V_{Ri}] = 0, \qquad f_i|_{t=0}(R,t) = f_{0i}, \quad (6)$$

$$\frac{\mathrm{d}(\bar{T}c_{pe}\rho_e)}{\mathrm{d}t} - 4\pi \sum_{i=1}^{2}\int_0^\infty f_i(R,t)J_{T,R,i}R^2\,\mathrm{d}R = 0, \qquad (7)$$

$$\sum_{i=1}^{2}L_iJ_{D,i} = \sum_{i=1}^{2}J_{T,R,i}, \qquad (8)$$

In order for system (6)–(8) to be solvable, it should be supplemented by the dependence of nucleus growth rate on the radius, V_{Ri}. Far from the eutectic point, the growth rate of nuclei is governed by heat conduction as well as diffusion [6]:

$$V_{Ri} = \frac{2\sigma_{SLi}D_{Le}\omega_i^2 N_0 T_{0i}K_{Le}\xi_{Ri}}{[\xi_{Ri}D_{Le}N_0L_i^2 + K_{Le}T_{0i}^2 k]R^2}\left(\frac{R}{R_{ci}} - 1\right), \qquad (9)$$

where D_{Le} is the coefficient of interdiffusion of components in a eutectic melt, N_0 is the total number of molecules per unit melt volume, k is the Boltzmann constant, σ_{SLi} is the energy of the liquid–solid interface, K_{Le} is the coefficient of heat conductivity of a eutectic melt, c_{pe}, and ρ_e are, respectively, the specific heat and density of the eutectic melt, ω_i is the volume per atom (molecule) of component i, L_i is the latent heat of crystallization per atom of component i and T_{0i} the equilibrium temperature.

In cases when the composition of a system is far from eutectic, the equilibrium concentration ξ_R is found from the asymptotic solution of Eqs. (6)–(8) and presents a real thermodynamic quantity, at which the Ostwald ripening comes to an end and the new phase equilibrates with the melt. Let us consider now the behavior of the growth rate V_{Ri} at the eutectic point. Let us apply the approach developed in Ref. [6] for a thermodynamically stable region to the domain of metastable states. The growth of nuclei of each phase is still described by Eq. (9). In this case ξ_{Ri} is the metastable equilibrium concentration [1–4]. It is the difference between the average concentration (which is equal to the eutectic concentration in the stage of Ostwald ripening) and the metastable equilibrium concentration that drives the growth of nuclei of the new phase. Just as in Ref. [6], the true equilibrium concentrations are determined from the asymptotic solution of Eqs. (1)–(5). This solution shows that the metastable equilibrium concentrations of each phase should be equal to one another, $\xi_{R1} = \xi_{R2}$, and to the actually observed equilibrium concentration ξ_e, i.e. to the eutectic concentration, and that the equilibrium temperatures are equal to the eutectic temperature, $T_{01} = T_{02} = T_e$. One

can therefore recast Eq. (9) for our case in the form:

$$V_{Ri} = \frac{2\sigma_{\mathrm{SL}i}D_{\mathrm{Le}}\omega_i^2 N_0 T_{\mathrm{e}} K_{\mathrm{Le}}\xi_{\mathrm{e}}}{[\xi_{\mathrm{e}}D_{\mathrm{Le}}N_0 L_i^2 + K_{\mathrm{Le}}T_{\mathrm{e}}^2 \mathrm{k}]R^2}\left(\frac{R}{R_{ci}} - 1\right) \qquad (10)$$

Thus, although the process of interest is driven by both thermal and diffusion processes, and the growth of nuclei can be rate-limited by diffusion, the supercooling reached in eutectic melts is the same for the entire system; it is this supercooling that is observable and measurable in a physical experiment.

We can see that Eqs. (6)–(8) and (10) describe the kinetics of crystallization of eutectic melts. It is known that $R_{ci} = 2\sigma_{\mathrm{SL}i}T_{0i}\omega_i/L_i\,\Delta_i T$, where T_{0i} is the equilibrium temperature and $\Delta_i T$ is the melt supercooling. Since the supercooling in the melt is the same for the two components, we have $R_{ci} = 2\sigma_{\mathrm{SL}i}T_{\mathrm{e}}\omega_i/L_i\,\Delta T$, and the critical radii of nuclei of different composition become similar, i.e. $R_{c1} = \gamma R_{c2}$, where $\gamma = \sigma_{\mathrm{SL}1}\omega_1 L_2/L_1\sigma_{\mathrm{SL}2}\omega_2$.

Thus, in the course of crystallization of a melt of eutectic composition the critical radii of nuclei of different kinds become similitude related. This implies that they vary in time by the same law.

Eqs. (6)–(9) are similar to the system describing Ostwald ripening in single-component melts [5], which is driven by a reduction of supercooling and the formation in the system of a generalized thermal field.

Thus Eqs. (6)–(9) relate to the late-stage evolution of an ensemble of new-phase nuclei of the compositions A and B. This system can be solved for $t \to \infty$ just as was done in Ref. [5].

For the distribution function of nuclei of each kind the solution gives:

$$f_i(R,t) = \frac{N_i(t)P_p(u)}{R_{ci}} \qquad (11)$$

where $p = 2, 3$ depends on the actual mechanism of heat and mass transport [6] involved, and $P_p(u)$ is the density of probability for a particle to have a dimension between u and $u + \Delta u$. We shall present the form of the distribution function $P_p(u)$ when discussing the evolution in open systems. The number of nuclei per unit volume varies in time as

$$N_i(t) = N_i(0)\left(\frac{A_{pi}t}{R_{c0i}^p}\right)^{-3/p}, \qquad (12)$$

where $N_i(0)$ is the number of nuclei species i at the onset of the Ostwald ripening process.

The evolution of the nucleus-critical radii in time for $t \to \infty$ obey the law:

$$R_{ci}^p \sim A_{pi}t, \qquad (13)$$

where A_{pi} are the transport coefficients whose values are available for all possible mechanisms of heat and mass transport [6]. In our case of conservative systems, the average, $\bar{R}_i$, and critical, R_{ci}, dimensions coincide. In

particular, for the mechanism of heat and mass transport specified $p = 3$, so that:

$$A_{3i} = \frac{8D_{\mathrm{Le}}\sigma_{\mathrm{SL}i}N_0\omega_i^2 T_{\mathrm{e}}\xi_{\mathrm{e}}K_L}{9(D_{\mathrm{Le}}L_i^2 N_{0i}\xi_{\mathrm{e}} + K_L T_{\mathrm{e}}^2)}. \qquad (14)$$

Since $R_{c1}(t) = \gamma R_{c2}(t)$, the nuclei of the compositions A and B have the same distribution function $P_p(u)$, and, accordingly, the functions $f_1(R,t)$ and $f_2(R,t)$ are mutually similar (see Eq. (11)). As follows from Eq. (13) for $t \to \infty$:

$$\frac{\sigma_{\mathrm{SL}i}\omega_i T_{\mathrm{e}}}{L_i\,\Delta T} = (A_{pi}t)^{1/p}. \qquad (15)$$

The ratio of the critical radii of nuclei of different species

$$\frac{\sigma_{\mathrm{SL}1}\omega_1 L_2}{\sigma_{\mathrm{SL}2}\omega_2 L_1} = \left(\frac{A_{p1}}{A_{p2}}\right)^{1/p} \qquad (16)$$

yields a significant relation between some coefficients. Indeed, in the case of $p = 3$ and

$$D_{\mathrm{Le}}L_i^2 N_0\xi_{\mathrm{e}} \ll K_L \mathrm{k}T_{\mathrm{e}}^2$$

we obtain from Eq. (16)

$$\frac{L_2}{L_1} = \left(\frac{\sigma_{\mathrm{SL}2}^2\omega_2}{\sigma_{\mathrm{SL}1}^2\omega_1}\right)^{1/3}, \qquad (17)$$

while for $D_{\mathrm{Le}}L_i^2 N_0\xi_{\mathrm{e}} \gg K_L \mathrm{k}T_{\mathrm{e}}^2$

$$\frac{L_2}{L_1} = \frac{\sigma_{\mathrm{SL}2}^2}{\sigma_{\mathrm{SL}1}^2}\frac{\omega_2}{\omega_1} \qquad (18)$$

If $p = 2$, i.e. if nucleus growth is rate-limited by the process of incorporation of atoms into the lattice, and the relation [5,6]

$$N_0\xi_{\mathrm{e}}\omega_i L_i \ll \mathrm{k}T_{\mathrm{e}},$$

holds, then

$$\frac{L_2}{L_1} = \left(\frac{\sigma_{\mathrm{SL}2}}{\sigma_{\mathrm{SL}1}}\frac{\omega_1}{\omega_2}\right)^{1/2}, \qquad (19)$$

while in the opposite case

$$\frac{L_2}{L_1} = \left(\frac{\sigma_{\mathrm{SL}2}}{\sigma_{\mathrm{SL}1}}\right)^{1/2} \qquad (20)$$

The expressions obtained above relate the latent heats of crystallization and surface tensions to volume per atom of the phases precipitating in eutectic melts. They allow us to predict the type of island growth mechanism which is characteristic of the system being studied. It enables to use these relations in order to refine the values of physical and chemical constants of the substances, e.g. surface tension. This suggests that the correlation between the nucleus radii brings about a kind of symmetry between the nucleus distributions in the late stages of crystallization. It is this process that is observed in the crystallization of normal eutectic, which reveals the onset of an orientation relation [2]. The experimental data shows, in particular, that at the onset of crystallization of Al–CuAl$_2$ alloys the components in the

Table 1
Compliance the reference data with the relations (17)–(20) (error in %)

System	Error (%)			
	Relation (17) (%)	Relation (18) (%)	Relation (19) (%)	Relation (20) (%)
Au–Ge	75	18	75	74
Pb–Sn	23	17	25	18
Bi–Sn	39	33	38	40

new phase appear to grow independently, whereas at the end of the process their growth is clearly interrelated. Note that the general nature of the above process extends also to nuclei of the new phase shaped as rods or cylinders, provided their radius R and length l vary in a correlated way. In this case we have to recast Eqs. (6)–(9) with due account of the change in the shape coefficient as was done in Ref. [7]. Solving the equation system we obtain the distribution functions of cylinders in size, similar to Eqs. (22) and (23), and expressions for cylinder length l and radius R, similar to Eq. (13). The approach suggested above can be employed for studies of melt crystallization in the eutectic point when a layer-by-layer mechanism proceeds. Then results of Refs. [8,9] and method developed here should be used. The character of the process is not changed dramatically but the relations (17)–(20) adopt a somewhat different form.

4. Evolution of an ensemble of nuclei taking into account a heat sink

Consider that the heat will be removed from the system where nuclei undergo Ostwald ripening in a melt of the eutectic composition. We shall assume the heat sinks to be of the volume type; in other words, the effect of nonuniformities associated with heat removal from the boundaries of the system will be neglected. At the stage of coalescence, the heat sinks can be described by the expression $g_T n t^{n-1}$, where g_T is the heat power and n is a damping index, which can be any number, not necessarily an integer [5]. For $n < 0 < 3/p$, the sinks are damped, while for $n \geq 3/p$ they are not damped [5]. In this study we are going to consider only damped heat sinks. Let us generalize Eqs. (6) and (7) to the case of evolution of an ensemble of nuclei at the eutectic point for an open system. The equation of continuity (6) will remain unchanged, whereas the equation of balance (7) should be supplemented by a heat sink. When considering the processes occurring at $t \to \infty$, we may drop the term $(d\bar{T}c_{pe}\rho_e/dt)$ since it is small compared to the heat sink. Thus, Eq. (7) should be put as follows:

$$g_T n t^{n-1} - 4\pi \sum_{i=1}^{2} \int_0^\infty f_i(R,t) J_{T,R,i} R^2 \, dR = 0,$$

The system (6)–(8) can be solved by the method described

in detail in Ref. [5]. We finally obtain, for the asymptotic size distribution function of nuclei of each species, the following expression:

$$f_i(R,t) = \frac{N_i(t) P_p(U)}{R_{ci}} \tag{21}$$

where

$$P_2(U) = \begin{cases} \dfrac{(2e)^{3-2n}(3-2n)U \exp\left(-\dfrac{3-2n}{1-U/2}\right)}{(2-U)^{2+2([3/2]n)}}, & U < 2 \\ 0, & U \geq 2 \end{cases} \tag{22}$$

$$P_3(U) =$$

$$\begin{cases} \dfrac{\left(\dfrac{3^3 e}{2^{5/3}}\right)^{1-n} 3(1-n)U^2 \exp\left[-\dfrac{(1-n)}{(1-2U/3)}\right]}{(U+3)^{1+[4/3(1-n)]}\left(\dfrac{3}{2}-U\right)^{2+[5/3(1-n)]}}, & U < 3/2 \\ 0, & U \geq 3/2 \end{cases} \tag{23}$$

where $U = (R/R_{ci})$. To return to closed systems, we should set $n = 0$ in Eqs. (22) and (23).

The density of nuclei varies as:

$$N_i(t) = \frac{N_i(0)}{(3/p - n)\left(\dfrac{A_{pi}}{R_{c0i}^p} t\right)^{(3/p-n)}} \tag{24}$$

The critical and average radii follow the relation

$$R_{ci}^p \sim A_{pi} t \qquad \bar{R}_i \sim R_{ci} C_{pn} \tag{25}$$

where C_{pn} is the coefficient defined in Ref. [5].

Thus we can see that Eqs. (21)–(25) coincide with the corresponding expressions of Ref. [5] within a constant thus implying that the basic features of Ostwald ripening also persist at the eutectic point.

5. Discussion of results

We have thus established that an evolution of the ensemble of new phase nuclei growing from the melt of the eutectic composition in the late ripening stage follows
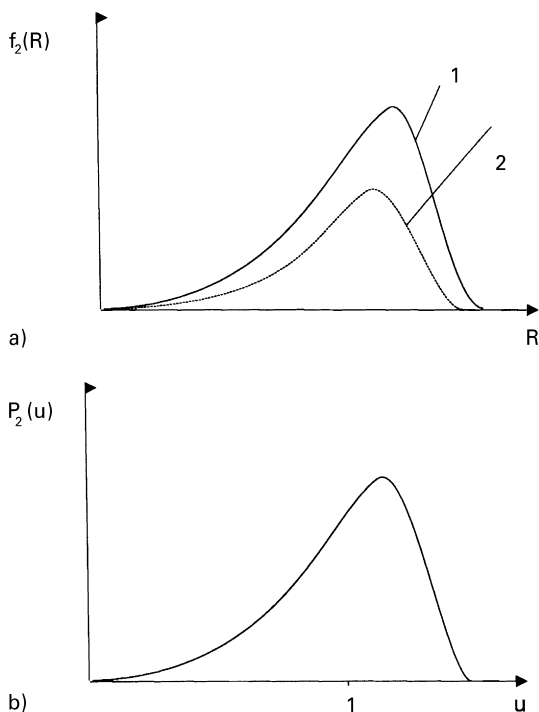
Fig. 2. The form of nuclei distribution function: (a) the size distribution function in dimension variables (Eq. (21)). The curve 1 is phase A, the curve 2 is phase B; and (b) the size distribution function in dimensionless variables R/R_{ci} Eq. (22). The distribution function is common for both phases.

the mechanism of "thermal" Ostwald ripening; i.e. it is driven by a reduction of the supercooling, ΔT, alone. The supercooling of the melt is the same for both phases and is reckoned from the temperature of the eutectic and the critical nucleus dimensions in both phases being connected by a similitude relationship. The ensembles of nuclei of different species follow a correlated evolution. In the stage of nucleation, the influence of each phase on the evolution of the other should be very weak. This conclusion is also supported by the experimental studies that show that the process of precipitation is usually started by one of the phases, called "leading". The mutual influence of the phases on their evolution becomes dominant in the later stage. Of particular interest are the relations (17)–(20) that stem from the correlation between the size distribution function of each phase. We should mention that these relations suggest that the nuclei of a new phase are spherical symmetric. Their validity can be demonstrated on the example of such eutectic systems as Au–Ge, Pb–Sn and Bi–Sn using reference data [10–12]. Substituting the reference data [10–12] into Eqs. (17)–(20) we calculated the discrepancy between the left and right hands which is tabulated (in %) in Table 1. The following values of constants were used in our calculations $L_{Bi} = 1.827 \times 10^{-20}$ J/at, $L_{Pb} = 7.794 \times 10^{-21}$ J/at, $L_{Sn} = 1.196 \times 10^{-20}$ J/at, $L_{Au} =$

2.09×10^{-20} J/at, $L_{Ge} = 6.235 \times 10^{-20}$ J/at; $\omega_{Bi} = 3.55 \times 10^{-30}$ m^3/at, $\omega_{Pb} = 3.025 \times 10^{-29}$ m^3/at, $\omega_{Sn} = 3.365 \times 10^{-29}$ m^3/at, $\omega_{Au} = 1.691 \times 10^{-29}$ m^3/at, $\omega_{Ge} = 2.262 \times 10^{-29}$ m^3/at; $\sigma_{Bi} = 6.02 \times 10^{-4}$ J/m^2, $\sigma_{Pb} = 4.6 \times 10^{-4}$ J/m^2, $\sigma_{Sn} = 5.9 \times 10^{-4}$ J/m^2, $\sigma_{Au} = 1.32 \times 10^{-4}$ J/m^2, $\sigma_{Ge} = 1.81 \times 10^{-4}$ J/m^2.

It should be noted that the exact constants needed for application of the relations (17)–(20) are usually unknown. It particularly refers to surface tension σ_{SL}. Its values given in Refs. [11,12] refer, as a rule, to "Solid/intrinsic melt" or "Solid A/Melt B" interphase energy while the relations we obtained require substitution of data for "solid/eutectic melt" interphase energy. As it is known such systems are difficult to measure, however, we can suggest that when intrinsic melt is replaced by the eutectic one σ_{SLi} changes to practically the same extent for both components. Then considering that we examine the ratio between constants we can use the values of "solid/intrinsic melt" interphase energy [11,12]. On the other hand, the relations (17)–(20) can be used for a more precise definition of the interphase energy values when the mechanism of heat mass transmission is determined. It may be done by the method given in Ref. [7].

We see that for the system Ge–Au Eq. (18) is the most satisfactory (error is 18%) and the limited stage is most likely the heat mass transfer. For Pb–Sn relations (18) and (20) fit to approximately equal accuracy but the condition $N_0 \xi_e \omega_i L_i \gg kT_e$ is not met; so the evolution is also determined by heat mass transfer. For this calculation we used the following constants [2,11,12]: $N_0 = 3.17 \times 10^{28}$ at/m^3, $\xi_e = 0.261$, $T_e = 456$ K. There is probably no primary heat mass transmission mechanism for the Bi–Sn system because neither relation fits to adequate accuracy. We have shown that the ensemble of nuclei undergoing Ostwald ripening at the eutectic point is characterized by a nucleus distribution in size that does not depend on the initial distribution function. Note that the distribution functions $P_p(u)$ of the two species of nuclei coincide in from if constructed in dimensionless variables $u = R/R_{ci}$, and are similar if written in dimensional ones (see Fig. 2). Most of the papers dealing with experimental investigation of eutectic melts either disregard the size distribution of nuclei altogether by restricting themselves to calculation of the average radius, or perform data treatment in dimensional variables [1–4]. As evident from this study, as well as from other works devoted to the theory of Ostwald ripening, a comprehensive interpretation of the processes involved (determination of the rate-limiting stage of nucleus growth, of the effect of heat sinks and of other parameters of the process on the final characteristics of a sample) requires the conversion of experimental data to dimensionless coordinates $u = R/R_{ci}$ and the processing of the results obtained by the technique described in Ref. [7].

The aforementioned discussion proves that the structure of samples of eutectic composition (in the sense of the particle size distribution) should be affected to a

considerable extent by the amount of heat removal from the system.

References

[1] R.W. Cahn, P. Haasen (Eds.), Physical Metallurgy, vol. 2, Elsevier, Amsterdam, 1983, p. 1957.

[2] R. Elliot, Eutectic Solidification Processing of Crystalline and Glassy Alloys, Butterworths, London, 1983, p. 309.

[3] M.Yu. Starostin, B.A. Gnesin, T.N. Yalovets, J. Cryst. Growth 171 (1997) 119.

[4] A. Hellawell, The Growth and Structure of Eutectics with Silicon and Germanium, Pergamon Press, New York, 1970, p. 78.

[5] S.A. Kukushkin, Acta Metallogr. Mater. 43 (1994) 715.

[6] S.A. Kukushkin, V.V. Slyozov, J. Phys. Chem. Solids 56 (1995) 1259.

[7] S.A. Kukushkin, V.V. Slyozov, J. Phys. Chem. Solids 57 (1996) 195.

[8] S.A. Kukushkin, T.V. Sakalo, Acta Metallogr. Mater. 41 (1993) 1237.

[9] S.A. Kukushkin, T.V. Sakalo, Acta Metallogr. Mater. 41 (1993) 1243.

[10] R.A. Lidin, L.L. Andreeva, V.A. Molochko, Constants of Inorganic Substances. A Handbook, Begell House, New York, 1995, p. 444.

[11] N. Eustathopoulos, Int. Metals Rev. 28 (4) (1983) 189.

[12] U.V. Naidich, V.M. Perevertailo, N.F. Gregorenko, Capillar Effects in the Processes of Growth and Melting of Crystals, Naukova Dumka, Kiev, 1983 (In Russian, p. 98).